Preliminary magnetostratigraphic results from the late Miocene Maragheh Formation, NW Iran

Salminen, Marja Johanna

2016

Salminen , M J , Paknia , M , Kaakinen , A P , Mirzaie Ataabadi , M , Zaree , G , Orak , Z & Fortelius , H L M 2016 , ' Preliminary magnetostratigraphic results from the late Miocene Maragheh Formation, NW Iran ' , Palaeobiodiversity and Palaeoenvironments , vol. 96 , no. þÿ 3 , pp. 433 443 . https://doi.org/10.1007/s12549-016-0239-y

http://hdl.handle.net/10138/234356
https://doi.org/10.1007/s12549-016-0239-y

acceptedVersion

Preliminary magnetostratigraphic results from the late Miocene Maragheh Formation, NW Iran

Johanna Salminen[1], Mohammad Paknia[2], Anu Kaakinen[2]*, Majid Mirzaie Ataabadi[3], Gholamreza Zare[4], Zahra Orak[5] and Mikael Fortelius[2]

[1]Department of Physics, P.O. Box 64, University of Helsinki, Finland
[2]Department of Geosciences and Geography, P.O. Box 64, University of Helsinki, Finland
[3]Department of Geology, University of Zanjan, Zanjan 45371/38791, Iran
[4]Department of Environment, Maragheh, Iran
[5]Department of Environment, National Museum of Natural History (MMTT), Tehran, Iran

*corresponding author

email: anu.kaakinen@helsinki.fi; tel. +358-2941 50819; FAX +358-2941 50827

Keywords

Fossil mammals, Maragheh fauna, Turolian, Paleomagnetism, Neogene, Iran, Hominoid

Abstract

Maragheh in northwestern of Iran is a world famous Miocene fossil-bearing area. The area has yielded classical late Miocene Turolian age fauna that has been collected and studied sporadically over the last 150 years. However, the precise correlation of these sediments to the Global Time Scale (GTS) has remained ambiguous. To address this, 115 levels along an approximately 27-m-thick interval were collected from the middle Maragheh Formation at Dareh Gorg (Gort Daresi) section. Characteristic remanent magnetization directions obtained by alternating field demagnetization produce a polarity pattern that is supported by thermal demagnetization on a set of sister specimens. Three polarity intervals were recognized, the middle part of the section at around 15–21 m showing reversed polarity, bounded by normal polarities above and below. Based on the paleontological constraints and recent K-Ar age determinations from the Maragheh Fm, three correlations to the geomagnetic polarity time scale appear likely. According to these correlations, recently discovered hominoid locality is correlated to C3Br.1n, C4n.1n, or to C4n.2n. For a unique correlation, however, additional paleomagnetic data is required from the upper and lower parts of the section.

Introduction

The Late Miocene (ca. 11.6–5 million years ago) is the time of the great expansion of the so-called "Pikermian" faunas in Eurasia, characterized by open-country adapted fossil mammal communities (Bernor et al. 1979, Bernor 1986; Eronen et al. 2009). Such animals including three-toed horses, giraffes, antelopes, rhinoceroses, elephants, big cats, hyenas, and many other smaller species roamed vast areas of Eurasia, from Spain and central-eastern Europe through the Balkans and Anatolia into the western and central Asia and China (Solounias et al. 1999; Agustí & Antón 2002). Maragheh, one of these localities, is a world famous fossil-bearing area and has been among the first localities with these faunas to be known and studied, along with Pikermi and Samos in Greece. The Maragheh fauna was first reported by a Russian explorer Khanikoff in 1840 (Bernor 1986, Bernor et al. 1996). The subsequent expeditions by different research groups extracted impressive fossil mammal collections, stored in several museums around the world (Mecquenem 1908, 1924–1925; Bernor 1978, 1986; Watabe 1990; Watabe & Nakaya 1991; Bernor et al. 1996; see Mirzaie Ataabadi et al. 2013 for details).

Correlation of the Maragheh sequence with the Global Time Scale is mainly achieved by a combination of radiometric dating techniques, including K-Ar (Erdbrink et al. 1976; Bernor et al. 1980; Campbell et al. 1980; Sawada et al. this issue), single grain crystal ^{40}Ar-^{39}Ar (Swisher III 1996) and fission track of zircons (Kamei et al. 1977; Bernor et al. 1980), and biostratigraphy. The interbedded lava flows, and ash beds and the mammalian faunas, especially the evolutionary stages of the *Hipparion* species, give a late Miocene age ranging from nearly 9 Ma to less than 7.6 Ma for the Maragheh fauna (Bernor et al. 1996; Mirzaie Ataabadi et al. 2013). However, the precise correlation of these sediments to the Global Time Scale (GTS) has remained ambiguous due to the error margins and partly due to inconsistence with stratigraphic division (Sawada et al. 2016, this issue).

Only preliminary paleomagnetism has previously been applied in the Maragheh area by the Dutch and Japanese groups who worked in the area in the 1970s (Erdbrink et al. 1976; Kamei et al. 1976). These analyses suggest that the samples in Maragheh show stable paleomagnetic results showing two magnetization polarities. However, only few levels were sampled; hence, reliable magnetostratigraphical correlations with the GTS based on these sparse data were not possible.

This study focuses on the late Miocene Maragheh Fm exposed in the Dareh Gorg. The volcanoclastic sediments of this interval comprise the middle part of the Maragheh Formation (Fig. 1). We sampled a large number of horizons from a well-exposed 27-m section for paleomagnetic study covering a recently discovered hominoid locality (Suwa et al. this issue). The objective of this study is to test whether a coherent magnetostratigraphic time framework can be achieved for the Maragheh Formation and secondly, to provide preliminary temporal framework and tie points for the Maragheh faunas and stratigraphic correlations. This is the first time that high-resolution magnetostratigraphy is employed to the classical Maragheh sequence.

Geological setting and stratigraphy

The Maragheh area belongs to the Hamedan-Tabriz (HTV) volcanic belt that trends in a NW-SE direction to the south of the Tabriz dextral fault (Anatolian transform fault). HTV belt was active in the Miocene to Quaternary and consists mainly of acidic andesite to dacite rocks (Azizi and

Moinevaziri 2009; Azizi et al. 2014). The late Miocene Maragheh sequence accumulated in the central part of the HTV, on the southern flank of the Mt. Sahand volcanic massif that forms a large calc-alcaline volcanic complex 100 km round (Bernor 1986; Azizi & Moinevaziri 2009). Kamei et al. (1977) named the entire 500–600-m-thick late Miocene sequence in the Maragheh basin as Maragheh Formation, whilst later work by Campbell et al. (1980) restricted the Maragheh Formation to the lowermost 300 m of volcanoclastic strata and separated the basal pyroclastic units as a Basal Tuff Formation, locally exceeding 80 m in thickness. The fossiliferous beds are concentrated to the lower half of the 300-m-thick Maragheh Formation, and they rest on the Basal Tuff Fm with a low angular unconformity. The whole sequence is capped by Pliocene-Quaternary terrace sediments, informally named as the Kerajek Formation. Campbell et al. (1980) and Bernor (1986) distinguished four sedimentary facies in the Maragheh Fm with poorly sorted massive siltstones comprising the bulk of deposits, pebble and cobble conglomerate, grey sandstone, and breccia, and air-fall tuff accounting for the less abundant facies.

Our fieldwork focused on the middle Maragheh Fm, in Dareh Gorg (Gort Daresi or “wolf valley”), located near Mordagh village ca. 15 km east-southeast from Maragheh town. Kamei et al. (1977) provided the first lithostratigraphical scheme for the Dareh Gorg section and described the distinctive marker beds above the Basal Tuff as Mordaq Tuff, Lower Pumice, White Fine Tuff, Upper Pumice, “Scoria” Bed, Pumice Falls, Sargizeh Tuff, and Korde Deh Ash Flow, that are the rudiments to the lithostratigraphic framework and correlation for this part of the Maragheh Formation. We follow Kamei et al. (1977) nomenclature modified by Sakai et al. (2016, figs 2 and 3, this issue). Sakai et al. (2016, this issue) conducted high-resolution facies analysis in Dareh Gorg and recognized nine lithofacies from the section, representing fluvial channel fills and flood plain facies associations. Our field investigations focused on the interval between the “hominoid locality” ca. 8 m below the “Middle Pumice” (Pumice Bed 2 of Mirzaie Ataabadi et al., 2013; likely the Lower Pumice of Kamei et al. 1977) and the White tuff (Fig. 2). The lithology of the studied interval shows a dominance of floodplain depositional environments (cf. Sakai et al. this issue), characterized by massive silty sand and sandy silt beds, commonly exhibiting paleosol formation and poorly sorted texture, and a few intercalated laminated silts. A notable feature is an up to 5-m-thick pumice bed (“the Middle Pumice”) comprised of stratified sand and pebble beds with occasional cobble-rich horizons in the lower part while the upper part mainly exhibits well-sorted laminated silts and fine sand. This unit has been interpreted as representing

hyperconcentrated flow deposits, likely to have been accumulated from a single flow (Sakai et al. this issue).

A large number of mammalian fossils have been found in the Dareh Gorg section, including the first known hominoid in Iran. In addition to the hominoid specimen, the lowermost part (hominoid locality or the "field museum site") of the studied interval has yielded proboscideans, rhinocerotids, bovids, equids, giraffes, hyaenids, and primates (Mirzaie Ataabadi et al. 2016, this issue). A fossil mammal site DRG1, recently excavated by the INSPE team (International Sahand Paleoenvironment Expedition), occurs below a coarse-grained channel fill deposit close to the "White Tuff" in the topmost part of the examined section. This unit has yielded equids and bovids, including three specimens of *Oioceros* sp., as well as few rhinos, carnivores, and cervids.

Sampling and magnetic measurements

Oriented paleomagnetic samples were collected from 115 levels along an approximately 27-m long section between the hominoid locality ("field station locality") and White tuff. A characteristic pumice layer "the Middle Pumice" formed a firm tie point between three subsections (Fig.1). All samples were derived from fresh surfaces exposed by digging trenches into the outcrop. Sampling focused on the fine-grained facies, coarse-grained beds were generally omitted; most of the samples were extracted from massive, relatively poorly sorted silt–fine sands beds, interpreted as representing debris flow and flood deposits on the floodplain (cf. Sakai et al. this issue). Average sampling spacing is 21 cm varying between 1 and 75 cm, excluding the two longer gaps that exist between ca 10.5 and 13.6 m due to poor outcrop conditions. The samples were taken with a gasoline-powered drill using water as a coolant and oriented with both magnetic and solar compasses. Drill core samples were cut in the laboratory to cylindrical specimens.

Magnetic measurements were carried out at the Solid Earth Geophysics Laboratory of the University of Helsinki, Finland. Stepwise alternating field (AF) demagnetizations were done using a three-axis demagnetizer with a maximum field of up to 160 mT, coupled with a 2G–DC SQUID magnetometer. A set of sister specimens were chosen for thermal demagnetization. These samples were first coated with sodium silicate and after that with mixture of MgO-ZrO_2 powder and water to prevent breaking during the heating. After the measurement of natural remanent magnetization

(NRM), samples were placed into liquid nitrogen in a null field to demagnetize viscous remanent magnetization (Borradaile et al. 2004), which removed 0–50% of the secondary remanence (0–15% of the total NRM). Thereafter, samples were thermally demagnetized to separate the characteristic remanent magnetization (ChRM) component by an argon-atmosphere ASC Scientific TD48-SC furnace. Magnetization after each step was measured using 2G–DC SQUID magnetometer. The AF method turned out to be more effective and provided more stable results than the thermal method. The demagnetization results were analyzed using orthogonal plots, stereographic projections, and demagnetization decay curves (Zijderveld 1967). Vector components were isolated using principal component analysis (Kirschvink 1980) and analyzed with Fisher (1953) statistics. Two quality filters for data were used. Data with calculated latitude of virtual geomagnetic pole (VGP) less than 30° were separated, because of the possibility of transitional geomagnetic field. In general, samples with maximum angular deviation (MAD) of 16° were rejected. If the data was not acceptable, a sister specimen from the same sample or from the same sampling level was measured if available.

Mass normalised susceptibility of all the samples was measured with a ZH Instruments company magnetic susceptibility meter using frequency of 1026 Hz and magnetic field of 320 A/m. Magnetic minerals were studied by thermomagnetic analysis of selected powdered whole rock specimens using an Agico KLY-3S-CS3 Kappabridge system. The low-temperature experiment, in which samples were heated from –192°C to room temperature (RT 25°C), was carried out first. Then, the same samples were heated from RT to 700°C and cooled back to RT in argon gas. Curie temperatures were determined using the Cureval 8.0 program (www.agico.com).

Results

Rock magnetic results

Susceptibility and NRM

Bulk magnetic susceptibilities (MS) are characterized by uniformly low values (mean 2.6×10^{-6} m^3/kg; Fig. 2) and very little scattering, except for the peak values (max. 13.8×10^{-6} m^3/kg) at the "Middle Pumice" level. The natural remanent magnetization (NRM) intensities vary between 1.1×10^{-2} and 3.1×10^{-1} mAm^2/kg for the entire section (Fig. 2). The highest NRM values (3.1×10^{-1} mAm^2/kg) were obtained for the floodplain deposits in the basal 5 m of the section whilst the "Middle Pumice bed" yields similar values with the bulk of the deposits.

Thermomagnetic properties

Thermomagnetic properties of the nine selected samples were measured. All the studied samples show irreversible heating and cooling curves (Fig 3). The majority of the samples show two ferromagnetic phases during the heating, first one with Curie temperatures between 550 and 580˚C indicating magnetite and a second one with Curie temperatures between 650 and 680˚C indicating hematite (Dunlop & Özdemir 1997). The sample 39A shows additional ferromagnetic phase at 380–400˚C that indicates titanomagnetite. Lower susceptibility of cooling curves shows that in spite of the argon atmosphere, some of the magnetite oxidised to hematite during heating. Low-temperature measurements show Verwey transition (Verwey 1939) between –157˚C and –175˚C for samples 90A, 19A, and 64A indicating the presence of stoichiometric magnetite.

Paleomagnetic results

The natural remanent magnetization (NRM) intensity decay curves after alternating field (AF) demagnetization show that the initial intensity decays rapidly to half of its original intensity with median destructive fields (MDF) less than 25 mT, so that for the 40% of the samples, MDF is less than 7.5 mT, pointing to magnetite as the dominant carrier of remanent magnetization. Progressive AF demagnetization reveals two components: an initial low coercivity component was obtained between 0 and 15 mT peak fields. A high coercivity characteristic remanent magnetization (ChRM) component was isolated between 15 and 120/160 mT with vector diagrams decaying to origin (Fig. 4) further supporting magnetite as the carrier of ChRM. However, since thermomagnetic analysis of samples show the presence of both magnetite and hematite, eleven samples were selected for thermal demagnetization in order to verify the carrier of ChRM. Intensity decay curves of thermal demagnetization show unblocking temperatures close to 580°C, supporting that magnetite carries the ChRM. Thermal demagnetization data also reveal two components. The low-temperature component is removed in temperatures less than 300°C and the high-temperature component is separated between 300°C and 580°C/640°C (Fig. 5). The maximum angular deviation (MAD) values for thermally demagnetized samples were less than 16° only for two samples.

Analyzed declination and inclination results are plotted in stratigraphic order in Fig. 2. In total, 143 specimens from 131 separate drill core samples were analysed. One hundred of these show well-defined ChRM directions with MAD less than 16° and are indicated with solid circles. Results from twenty-three specimens show VGP latitude less than 30°, which could indicate transitional geomagnetic field and are indicated with a white triangle. In addition, twenty specimens show MAD values higher than 16° and are plotted with a grey square, but seventeen of these show otherwise clear polarities (Fig. 2).

All the ChRM directions obtained are shown in the Fig. 6. Paleomagnetic reversal test was used to determine whether the average normal and reversed NRM directions are statistically antipodal within a given confidence limit (McFadden & McElhinny 1990). The mean direction for seventy-eight normal samples is D= 356.5°, I= 45.4° with α95= 5.9°, K= 8.3, and R= 68.7, and the mean direction for twenty-two reversed samples is D= 171.7°, I= -47.7° with α95=17.5°, K= 4.3, and R= 16.3 (Fig. 6). The test shows that the antipode of the mean of the reversed polarity sites and the mean of the normal polarity sites pass the test with classification Rc (observed angle is 4.0° and critical angle in 14.8°). Passage of the reversal test indicates that ChRM directions do not have contamination due to secondary magnetization.

Discussion and conclusions

Previous paleomagnetic studies

Two previous paleomagnetic studies have been carried out for the Maragheh Formation in 1970s by Erdbrink et al. (1976) and Kamei et al. (1977). Erdbrink et al. (1976) sampled different tuffaceous and other volcanic layers at ten levels along a 79.5-m composite section in Maragheh. The samples were subjected to alternating field demagnetization with maximum fields of 300 mT for test samples and 150 mT for rest of the samples. Seven horizons provided reliable results showing normal polarities for the lowermost samples and reversed polarities for the overlying levels. Kamei et al. (1977) further continued paleomagnetic studies by sampling nine levels at Dareh Gorg section from coarse biotite tuff below the Ignimbritic tuff (Mordaq) and spanning up to Korde deh ash flow far above the Upper pumice. According to Kamei et al. (1977), reasonable results were obtained from four sites: a reversed polarity from the coarse Biotite tuff below the Ignimbritic tuff and normal polarities for the Ignimbritic tuff, White fine tuff, and for Korde deh ash flow. However, our results show that the 8 mT alternating field demagnetization used by

Kamei et al. (1977) does not adequately separate ChRM magnetization component, since some of the samples required fields up to 15 mT to clean the viscous component. Therefore, the obtained normal polarities in Kamei et al. (1977) may represent the direction of the present Earth's magnetic field at the sampling site (*D*: 50.5°, *I*: 56.9°). Based on these sparse paleomagnetic data, it was not possible to draw any conclusions about the age of the section, but they nevertheless demonstrate that the material is suitable for paleomagnetic study.

Paleomagnetism and magnetozones

Two magnetization components were obtained during the paleomagnetic analyses. First one is a low coercivity and a low-temperature viscous component and the second one is a higher coercivity and a high-temperature characteristic remanent magnetization component (ChRM) carried by nearly stoichiometric magnetite in majority of the studied samples. This is evidenced by median destructive fields less than 20 mT for majority of the samples, unblocking temperatures of 580°C, Curie temperatures between 550°C and 580°C, and obtained Verwey transitions. Based on the obtained polarities, three magnetozones can be defined (Fig. 2). The base of the section (0–13.6 m), including the Middle Pumice, shows a normal polarity while the magnetization of overlying samples at 13.60 to 14.30 m show unstable and at 14.30 to 15.15 m transitional field from normal to reversed polarity. A reversed polarity occurs at the 15.55–20.65-m level and the uppermost interval up to the White tuff comprises of normal polarity.

Earlier geochronology and correlation of magnetozones to the ATNTS

Different Pumice beds of Maragheh Formation have been dated by fission track of zircons (Kamei et al. 1977; Bernor et al. 1980) by K-Ar using plagioclase and hornblende (Erdbrink et al. 1976; Bernor et al. 1980; Campbell et al. 1980; Sawada et al. 2016, this issue) and by ^{40}Ar-^{39}Ar using plagioclase (Swisher III 1996). These individual radiometric age determinations with their error limits are shown in Figure 7 and Table 1 and discussed briefly here for correlating the obtained magnetozones, but more extensively by Sawada et al. (2016, this issue). Erdbrink et al. (1976) provided K-Ar age of 12.9 ± 0.7 Ma for the Ignimbritic tuff and age of 2.5 ± 0.5 Ma for the uppermost part of the Maragheh Formation. Later, this range of 10 Myr in ages for the Maragheh formation has been narrowed down to ca. 2 Myr using K-Ar (Bernor et al. 1980; Campbell et al. 1980; Sawada et al. this issue), fission track (Kamei et al. 1977; Bernor et al. 1980), and ^{40}Ar-^{39}Ar ages (Swisher III 1996).

The recently obtained mean value of hornblende and plagioclase ages of Sawada et al. (2016, this issue) bracket the Mordaq tuff to 8.41–7.87 Ma. The mean values of mineral ages of the Lower Pumice Beds are 7.54 ± 0.22 Ma (A) and 6.95 ± 0.28 Ma (B), and of the Upper Pumice 6.96 ± 0.31 Ma. The mean hornblende and plagioclase K-Ar age of the Middle Pumice (7.87 ± 0.29Ma) is older than those for the Lower Pumice and therefore not consistent with the stratigraphy. Based on similar geochemical major and trace element composition in the two marker beds, Sawada et al. (2016, this issue) suggest that pumices of the Middle Pumice bed are reworked from the underlying Lower Pumice unit and the ages do not represent the accumulation age of the Middle Pumice. Previous fission track (FT) zircon ages of Kamei et al. (1977) for Dareh Gorg section range slightly younger ages for the marker beds but with larger error limits suggesting 8.4–5.6 Ma for the Ignimbritic tuff (Mordaq tuff), 7.8–5.2 Ma for the Lower Pumice (possibly corresponds to the Middle Pumice in our study; Mirzaie Ataabadi et al. 2016, this issue), and 7.9–5.3 Ma for the Upper Pumice. In addition to large errors, these earlier fission track ages are subject to larger uncertainties by default since the FT method has developed substantially since 1990, yet still facing the problem of absolute age calibration (e.g. Turner et al. 1980; Gallagher et al. 1998; Danhara and Iwano 2013). Since the radiometric age of Sawada et al. (2016, this issue) is acquired using recent K-Ar technology on two different minerals and with lower error limits than in previous studies, we base our correlation on these recent ages.

Using the maximum (minimum) mean mineral K-Ar age for the Lower Pumice (Upper Pumice) (Fig. 7) and the biostratigraphical evidence (Bernor et al. 1996; Mirzaie Ataabadi et al. 2013), we consider a correlation of our magnetostratigraphic column to the Astronomically Tuned Neogene Time Scale (ATNTS) of Gradstein et al. 2012 (Fig. 2). K-Ar results (Sawada et al. 2016, this issue) provide an approximate maximum age of 7.76 Ma for the Lower Pumice and a minimum age of 6.65 Ma for the Upper Pumice. These age constraints and the pattern of magnetozones allow several possible correlations for the polarity sequence. According to these options, the polarity sequence correlates between the (upper part of) chron C4n.2n and (lower part of) chron C3An.2n. Consequently, the reversal could be connected to C4n.1r, C3Br.3r, C3Br.2r, C3Br.1r, or C3Ar. While all correlations appear possible, we prefer placing the reversed polarity zone to C4n.1r (option 1), C3Br.3r (option 2), or C3Br.1r (option 3). The resultant sedimentation accumulation rates for the reversed chrons are approximately 11–15 cm/ka, agreeing well with the estimated

sedimentation rate of 12.5cm/ka by Mirzaie Ataabadi et al. (2013). These correlations imply that the hominoid locality would fall in the upper part of normal chron 4n.2n (option 1), 4n.1n (option 2), or in 3Br.1n (option 3). Placing the reversed polarity zone to 3Br.2r or 3Ar would result in much lower sedimentation rates (approximately 3.5 and 1.5 cm/ka, respectively) and are considered less likely. Nevertheless, the accumulation rate in Maragheh is based on one magnetochron only, and large variation in rates through the sequence is expected. We also ackowledge that additional paleomagnetic data from the lower and upper part of the section is still required to extend the section for a firmer correlation.

Conclusions

First high-resolution paleomagnetic results from the classical Maragheh sequence in NW Iran provide a preliminary magnetostratigraphy for the middle Maragheh Formation in Dareh Gorg section. The quality of demagnetization results on which the magnetostratigraphic pattern is based is of high quality for both normal and reversed samples, and three polarity intervals are recognized. Our magnetostratigraphic correlation suggests placing the recently discovered hominoid locality to the upper part of the normal polarity chron C4n.2 (7.695–8.108 Ma), chron C4n.1n (7.528–7.642 Ma), or C3Br.1n (7.251–7.285 Ma). We acknowledge, however, that we can only propose a tentative correlation with the geological time scale. For a unique correlation, a distinct reversal pattern is necessary.

Acknowledgments

Department of Environment (environment protection organization), the Government of Iran permitted and facilitated this study. We would like to express our gratitude to the heads of the "natural environment division" of this organization as well as those of the "office of natural history museum and genetic resources" and East Azarbaijan and Maragheh branches for their support. We thank field assistance by Mr. Mohammad Ali, Mr. Suleiman Zadeh, and Ms. Mansoureh Hasandoost and members of the INSPE (International Sahand Palaeoenvironmental Expedition) team. This paper benefited significantly from constructive suggestions from Sevket Sen, Miguel Garcés, Elisabet Beamud Amorós, and the Editor-in-chief Peter Königshof. Field work in

Maragheh was partially supported by the Academy of Finland (project no 257850 and 264935), RHOI project, Sasakawa Foundation, and Nordenskiöld samfundet.

Conflict of Interest: The authors declare that they have no conflict of interest.

References

Agustí, J., & Antón, M. (2002). Mammoths, sabertooths, and hominoids: 65 million years of mammalian evolution in Europe. New York: Columbia University Press, 313 pp.

Azizi, H., & Moinevaziri, H. (2009). Review of the tectonic setting of Cretaceous to Quaternary volcanism in northwestern Iran. Journal of Geodynamics, 47(4), 167–179.

Azizi, H., Asahara, Y., Tsuboi, M., Takemura K., & Razyani, S. (2014). The role of heterogenetic mantle in the genesis of adakites northeast of Sanandaj, northwestern Iran. Chemie der Erde, 74(1), 87–97.

Bernor, R. L. (1978). The Mammalian systematics, biostratigraphy and biochronology of Maragheh and its importance for understanding late Miocene Hominoid Zoogeography and Evolution. Los Angeles: University of California Dissertation.

Bernor, R. L. (1986). Mammalian biostratigraphy, geochronology and zoogeographic relationships of the late Miocene Maragheh fauna, Iran. Journal of Vertebrate Paleontology 6 (1), 76–95.

Bernor, R. L, Andrews, P. A., Solounias, N., van Couvering, J. A. (1979). The evolution of "Pontian" mammal faunas: some zoogeographic, palaeoecological, and chronostratigraphic considerations. The VIIth Inter Congr Medit Neogene. Annales géologiques des Pays helléniques hors-série, I, 81–89.

Bernor, R. L., Woodburne, M. O., & Van Couvering, J. A. (1980). A contribution to the chrolonology of some old world Miocene faunas based on Hipparionine Horses. Geobios, 13 (5), 705–739.

Bernor, R. L., Solounias, N., Swisher C. C. III, & van Couvering, J. A. (1996). The correlation of three classical “Pikermian” mammal faunas — Maragheh, Samos, Pikermi — with the European MN Unit System. In R.L. Bernor, V. Fahlbusch & H.-W. Mittman (Eds), The evolution of western Eurasian Neogene mammal faunas (pp. 137–154). New York: Columbia University Press.

Borradaile, G. J., Luca, K., & Middleton, R. S. (2004). Low-temperature demagnetization isolates stable magnetic vector components in magnetite-bearing diabase. Geophysical Journal International 157 (2), 526–536.

Campbell, B. G., Amini, M. H., Bernor, R. L., Dickinson, W., Drake, R., Morris, R., Van Couvering, J.A., & Van Couvering, J.A.H. (1980). Maragheh: a classical late Miocene vertebrate locality in northwestern Iran. Nature, 287 (5785), 837–841.

Danhara, T., & Iwano, H. (2013). A review of the present state of the absolute calibration for zircon fission track geochronometry using the external detector method. Island Arc, 22, 264–279.

de Mecquenem, R. (1908). Contribution à l’étude du gisement des vertebrés de Maragha et ses environs. In J. Morgan de (Ed.), Délégation scientifique en Perse. Annales d’Histoire Naturelle, I, Paléontologie, 27–79.

de Mecquenem, R. (1924). Contribution à l’étude des fossiles de Maragha. Annales de Paléontologie, 13/14, 133–160.

Dunlop, D. J., & Özdemir, Ö. (1997). Rock Magnetism: fundamentals and frontiers (p. 573). Cambridge: Cambridge University Press.

Erdbrink, D. P. B., Priem, H. N. A., Hebeda, E. H., Cup, C., Dankers, P., & Cloetingh, S. A. P. L. (1976). The bone bearing beds near Maragheh in N.W. Iran. Geology Series B, 79(2), 85–113.

Eronen, J. T., Mirzaie Ataabadi, M., Micheels, A., Karme, A., Bernor, R. L., & Fortelius, M. (2009). Distribution history and climatic controls of the Late Miocene Pikermian chronofauna. Proceedings of the National Academy of Sciences, USA, 106(29), 11867–11871.

Fisher, R. (1953). Dispersion of a sphere. Proceedings of the Royal Society of London, 217 (1130), 295–305.

Gallagher, K., Brown, R., & Johnson, C. (1998). Fission track analysis and its applications to geological problems. Annual Reviews of Earth and Planetary Science, 26, 519–572.

Gradstein, F. M., Ogg, J. G., Schmitz, M. D., & Ogg, G. M. (2012). The geologic time scale. Amsterdam: Elsevier.

Kamei, T., Ikeda, J., Ishida, H., Ishida, S., Onishi, I., Partoazar, H., Sasajima, S., & Nishimura, S. (1977). A general report of the geological and paleontological survey in Maragheh area, North-West Iran. Memoirs of the faculty of science, Kyoto University, Series of Geology and Mineralogy, XLIII (1/2), 131–143.

Kirschvink, J. L. (1980). The least-squares line and plane and the analysis of palaeomagnetic data. Geophysical Journal of the Royal Astronomical Society, 62 (3), 699–718.

McFadden, P. L., & McElhinny, M. W. (1990). Classification of the reversal test in palaeo-magnetism. Geophysical Journal International, 103(3), 725–729.

Mirzaie Ataabadi, M., Bernor, R. L., Kostopoulos, D., Wolf, D., Orak, Z., Zare, G., Nakaya, H., Watabe, M., & Fortelius, M. (2013). Recent advances on paleobiological research of the late Miocene Maragheh fauna, northwest Iran. In X. Wang, M. Fortelius, & L. Flynn (Eds.), Asian Neogene mammal biostratigraphy and chronology (pp.544–563). New York: Columbia University Press.

Mirzaie Ataabadi, M., Kaakinen, A., Kunimatsu, Y., Nakaya, H., Orak, Z., Paknia, M., Sakai, T., Salminen, J., Sawada, Y., Sen, S., Suwa, G., Watabe, M., Zare, G., Zhang, Z., & Fortelius, M., (2016). The late Miocene hominoid-bearing site in Maragheh Formation, Northwest Iran. In M. Mirzaie Ataabadi and M. Fortelius (Eds.), The late Miocene Maragheh mammal fauna; results of

recent multidisciplinary research. Palaeobiodiversity and Palaeoenvironments, 96(3). Doi: 10.1007/s12549-016-0241-4

Sakai, T., Zaree, G., Sawada, Y., Mirzai Ataabadi, M., & Fortelius, M. (2016). Depositional environment reconstruction of the Maragheh Formation, East Azarbaijan, Northwestern Iran. In M. Mirzaie Ataabadi and M. Fortelius (Eds.), The late Miocene Maragheh mammal fauna; results of recent multidisciplinary research. Palaeobiodiversity and Palaeoenvironments, 96(3) Doi: 10.1007/s12549-016-0238-z

Sawada, G., Zaree, G., Sakai, T., Itaya, T., Yagi, K., Hyodo, H., Imaizumi, M., Mirzaie Ataabadi, M., & Fortelius, M. (2016). K-Ar ages and petrology of the late Miocene pumices from the Maragheh Formation, northwest Iran. In M. Mirzaie Ataabadi and M. Fortelius (Eds.), The late Miocene Maragheh mammal fauna; results of recent multidisciplinary research. Palaeobiodiversity and Palaeoenvironments, 96(3) DOI: 10.1007/s12549-016-0232-5

Solounias, N., Plavcan, J. M., Quade, J. & Witmer, L. (1999). The paleoecology of the Pikermian Biome and the savanna myth. In J. Agustí, L. Rook, & P. Andrews (Eds.), The evolution of Neogene terrestrial ecosystems in Europe (pp 436–453).Cambridge: Cambridge University Press.

Suwa, G., Kunimatsu, Y., Mirzai Ataabadi, M., Orak, Z., Sasaki, T. and Fortelius, M. (2016). The first hominoid from the Maragheh Formation, Iran. In M. Mirzaie Ataabadi and M. Fortelius (Eds.), The late Miocene Maragheh mammal fauna; results of recent multidisciplinary research. Palaeobiodiversity and Palaeoenvironments, 96(3) Doi: 10.1007/s12549-016-0234-3

Swisher, C. C., III (1996). “New 40Ar/39Ar dates and their contribution toward a revised chronology for the late Miocene of Europe and west Asia. In R. L. Bernor, V. Fahlbusch & H. W. Mittmann (Eds.), The evolution of western Eurasian Neogene mammal faunas (pp. 64–77). New York: Columbia University Press.

Turner, D. L., Triplehorn, D. M., Naesser, C. W., & Wolfe, J. A., 1980. Radiometric dating of ash partings in Alaskan coal beds and upper Tertiary paleobotanical stages. Geology, 8, 92–96.

460 Verwey, E. J. W. (1939). Electronic conduction of magnetite (Fe_3O_4) and its transition point at low
461 temperatures. Nature, 144(3642), 327–328.
462
463 Watabe, M. (1990). Fossil bovids (Artiodactyla, Mammalia) from Maragheh (Turolian, late
464 Miocene), Northwest Iran. Annual Report Historical Museum Hokkaido, 18, 19–55.
465
466 Watabe, M. & Nakaya, H. (1991). Phylogenetic significance of the postcranial skeletons of the
467 hipparions from Maragheh (Late Miocene), Northwest Iran. Memoirs of the Faculty of Science,
468 Kyoto University, Series of Geology & Mineralogy, 56 (1–2), 11–53.
469
470 Zijderveld, J. D. A. (1967). A.C. demagnetization of rocks: analysis of results. In: D. W. Collinson,
471 K. M. Creer, & Runcorn, S. K. (Eds.), Methods in paleomagnetism (pp. 254–286). Elsevier,
472 Amsterdam
473

Figure captions

Figure 1. a – Satellite image (Google Earth) of the study area. b – The study site at Dareh Gorg and the sampled subsections a–c. The Middle Pumice and the underlying paleosol were used as marker beds in lithostratigraphical correlation

Figure 2. Lithological column, natural remanent magnetization (*NRM*), magnetic susceptibility, declination (*Decl*) and inclination (*Incl*) of characteristic remanent component and interpreted magnetostratigraphic polarity for Maragheh. In the polarity column, *black (white)* denotes normal (reversed) polarity. *Grey shaded zones* represent transitional or undefined polarity. Positions of Middle Pumice (*MP*), White Tuff (*WT*), and fossil localities are indicated. Suggested correlations of the magnetostratigraphy of the middle Maragheh Fm to the Astronomically Tuned Neogene Time Scale (*ATNTS*) of the geological time scale 2012 (Gradstein et al. 2012) together with minimum and maximum mean mineral K-Ar ages for the Upper Pumice (*UP*) and Lower Pumice (*LP*) (cf. Sawada et al. 2016, this issue) are shown on the right column

Figure 3. Thermomagnetic curves (susceptibility vs. temperature) for samples from different lithologies at the Maragheh. Specimens were heated from room temperature up to 700°C (*red, solid curve*) and cooled back to room temperature (*blue, dotted curve*) in argon gas

Figure 4. Examples of demagnetization behaviour during alternating field (AF) demagnetization. Shown are orthogonal (Zijderveld, 1964) demagnetization diagrams. *Solid (open) symbol*s refer to the projection on the horizontal (vertical) plane in geographic coordinates. Number at demagnetization step denotes the AF value in mT

Figure 5. Examples of demagnetization behaviour during thermal (TH) demagnetization. Shown are orthogonal (Zijderveld 1964) demagnetization diagrams (in *left side*) and intensity decay curve (in *right side*). *Solid (open) symbols* refer to the projection on the horizontal (vertical) plane in geographic coordinates. Number at demagnetization step denotes the TH value in °C

Figure 6. Equal area projection of characteristic remanent magnetization directions for Maragheh. *Solid (open) symbols* are directions in the lower (upper) hemisphere. The means are shown with

stars with circle of 95% confidence. The antipode of the mean of the reversed polarity sites is within 4° of the mean of the normal polarity site. Data pass the reversal test of paleomagnetic stability (McFadden and McElhinny 1990)

Figure 7. Radiometric ages and magnetostratigraphic polarities for the Dareh Gorg section obtained in the earlier studies of Kamei et al. (1977); Bernor et al. (1980); Swisher III (1996); Sawada et al. (2016), this issue. Dated key beds are drawn in stratigraphical order. The 27-m long section sampled in this study, and the location of field station is indicated in the column

Table captions

Table 1. Radiometric ages obtained for the Dareh Gorg section

Table 1 Radiometric ages obtained for the Dareh Gorg section.

Method (mineral)	S	**Ignimbritic tuff** Age (Ma)	**Lower Pumice** Age (Ma)	**Middle Pumice** Age (Ma)	**Upper Pumice** Age (Ma)	**Reference**
Fission track (zircon)	△	7.0 ± 1.4		6.5 ± 1.3[a]	6.6 ± 1.3	Kamei et al. 1977
K-Ar (pl)	□	8.9 ± 0.5 8.8 ± 0.5 6.4 ± 0.5				Bernor et al. 1980
Fission track	▲	10.6 ± 0.8				Bernor et al. 1980
Ar-Ar (pl)	●	8.645 ± 0.029				Swisher III et al. 1996
K-Ar mean (hbl, pl)	■	8.14 ± 0.27	7.54 ± 0.22 6.95 ± 0.28	7.87 ± 0.29	6.96 ± 0.31	Sawada et al. 2016 this volume (mean)

S symbol in Fig.7., *hbl* hornblende, *pl* plagioclase

[a] Lower Pumice of Kamei et al. (1977)

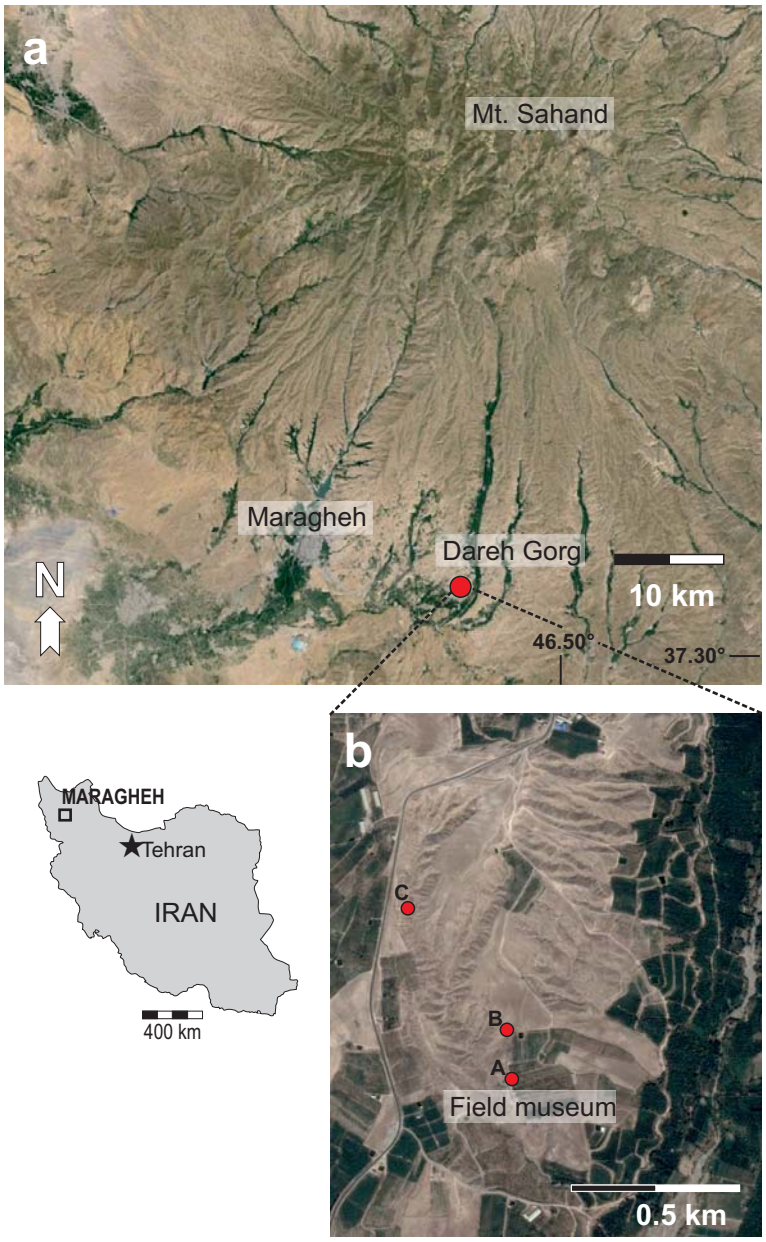
a
Mt. Sahand
Maragheh
Dareh Gorg
10 km
N
46.50°
37.30°
MARAGHEH
Tehran
IRAN
400 km
b
C
B
A
Field museum
0.5 km

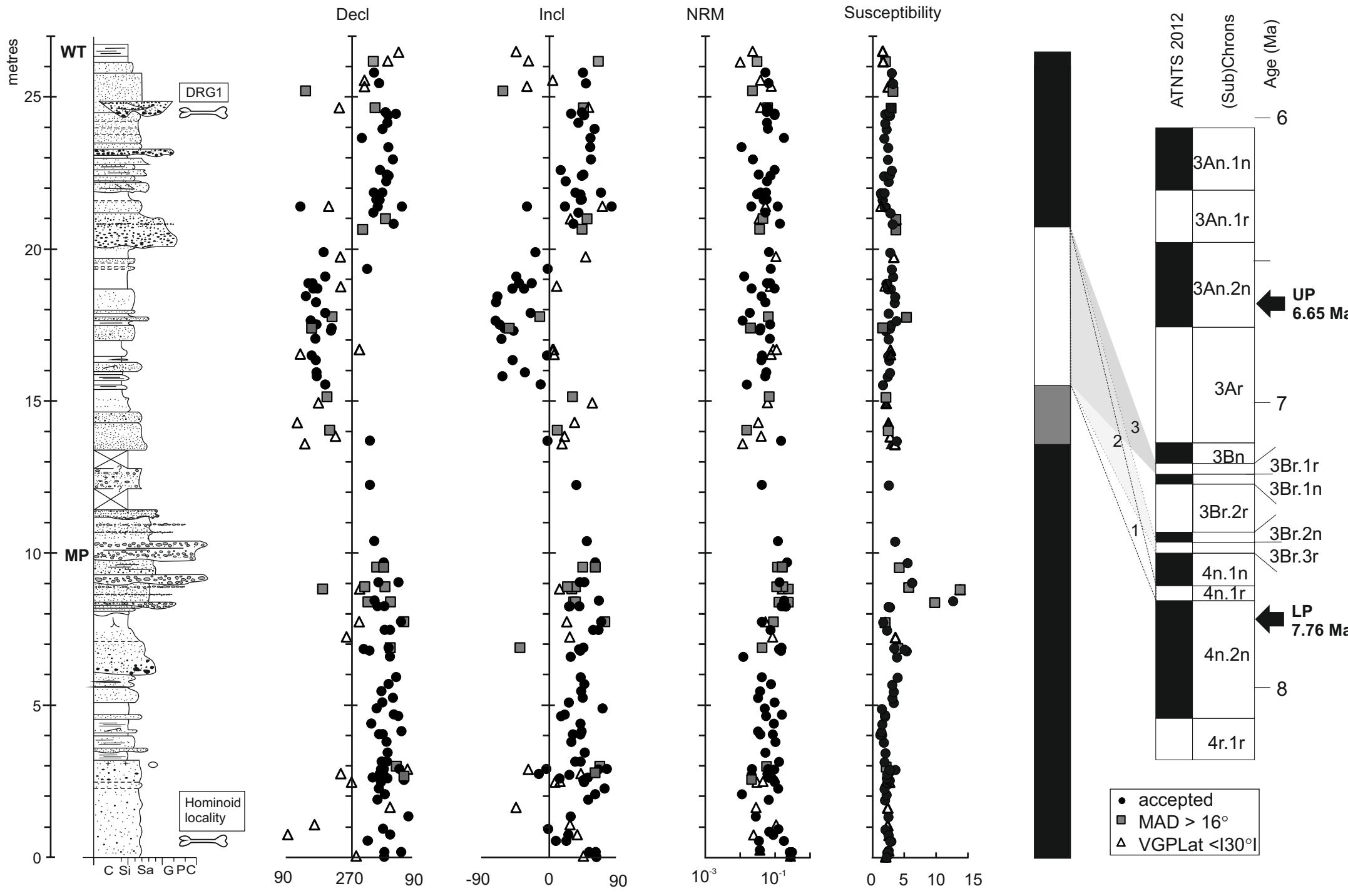
metres
WT
MP
DRG1
Hominoid locality
C Si Sa G P C
Decl
Incl
NRM
Susceptibility
90 270 90
-90 0 90
10^{-3} 10^{-1}
0 5 10 15
ATNTS 2012
(Sub)Chrons
Age (Ma)
3An.1n
3An.1r
3An.2n
3Ar
3Bn
3Br.1r
3Br.1n
3Br.2r
3Br.2n
3Br.3r
4n.1n
4n.1r
4n.2n
4r.1r
UP
6.65 Ma
LP
7.76 Ma
1
2
3
accepted
MAD > 16°
VGPLat <|30°|

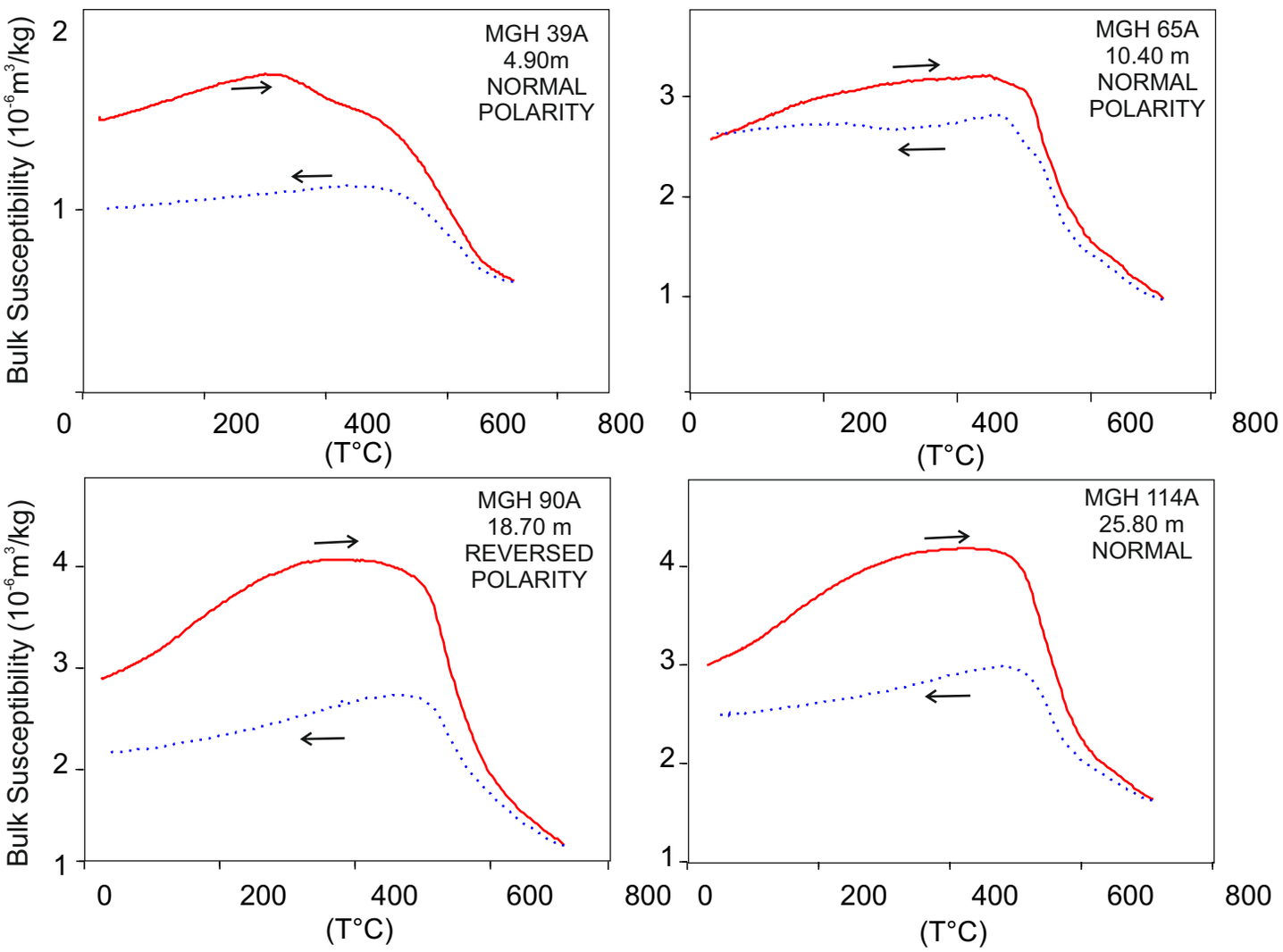
Bulk Susceptibility ($10^{-6}m^3/kg$)
MGH 39A
4.90m
NORMAL
POLARITY
MGH 65A
10.40 m
NORMAL
POLARITY
MGH 90A
18.70 m
REVERSED
POLARITY
MGH 114A
25.80 m
NORMAL
(T°C)
0
200
400
600
800

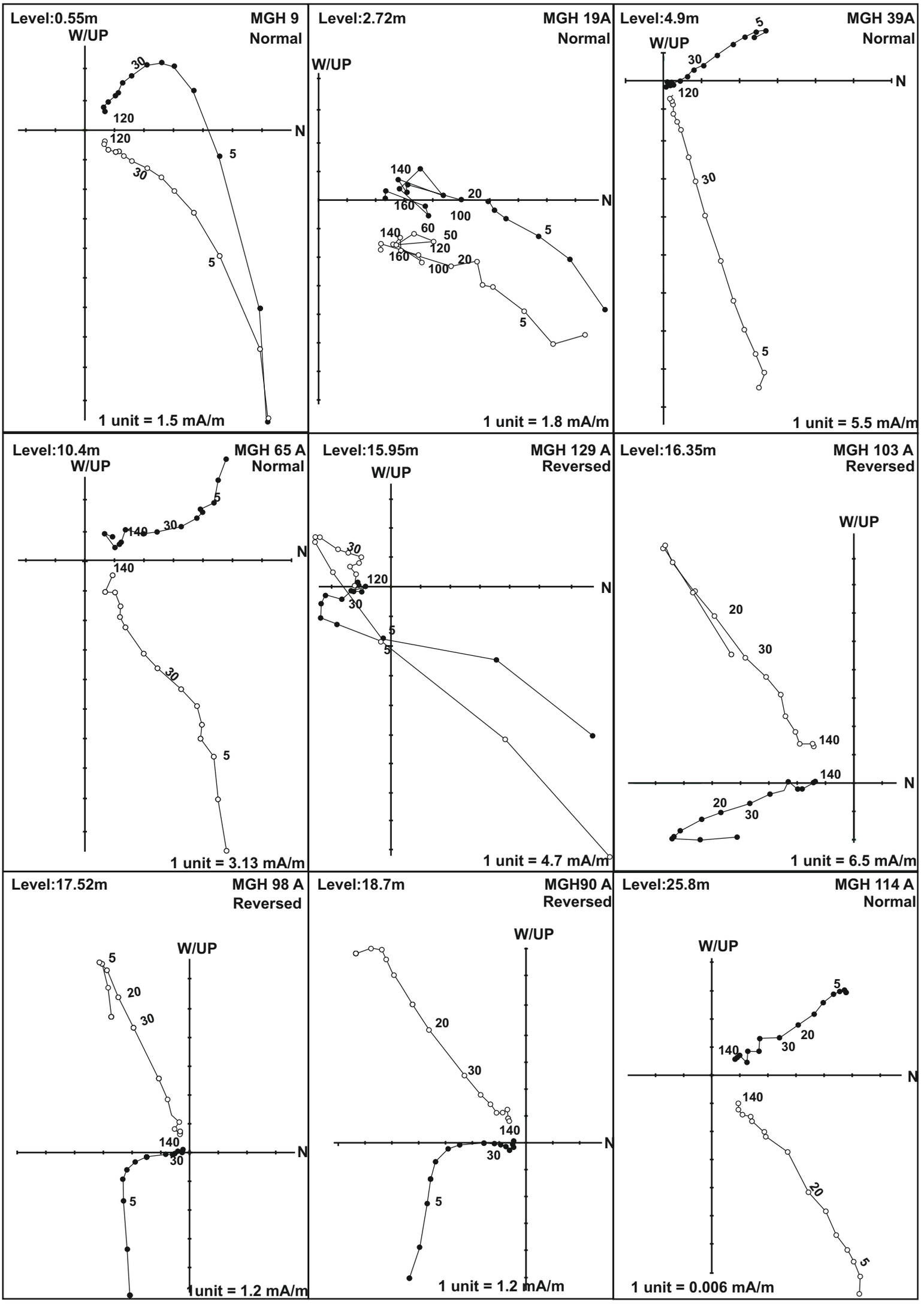
Level:0.55m
MGH 9
Normal
W/UP
N
1 unit = 1.5 mA/m
Level:2.72m
MGH 19A
Normal
W/UP
N
1 unit = 1.8 mA/m
Level:4.9m
MGH 39A
Normal
W/UP
N
1 unit = 5.5 mA/m
Level:10.4m
MGH 65 A
Normal
W/UP
N
1 unit = 3.13 mA/m
Level:15.95m
MGH 129 A
Reversed
W/UP
N
1 unit = 4.7 mA/m
Level:16.35m
MGH 103 A
Reversed
W/UP
N
1 unit = 6.5 mA/m
Level:17.52m
MGH 98 A
Reversed
W/UP
N
1unit = 1.2 mA/m
Level:18.7m
MGH90 A
Reversed
W/UP
N
1 unit = 1.2 mA/m
Level:25.8m
MGH 114 A
Normal
W/UP
N
1 unit = 0.006 mA/m

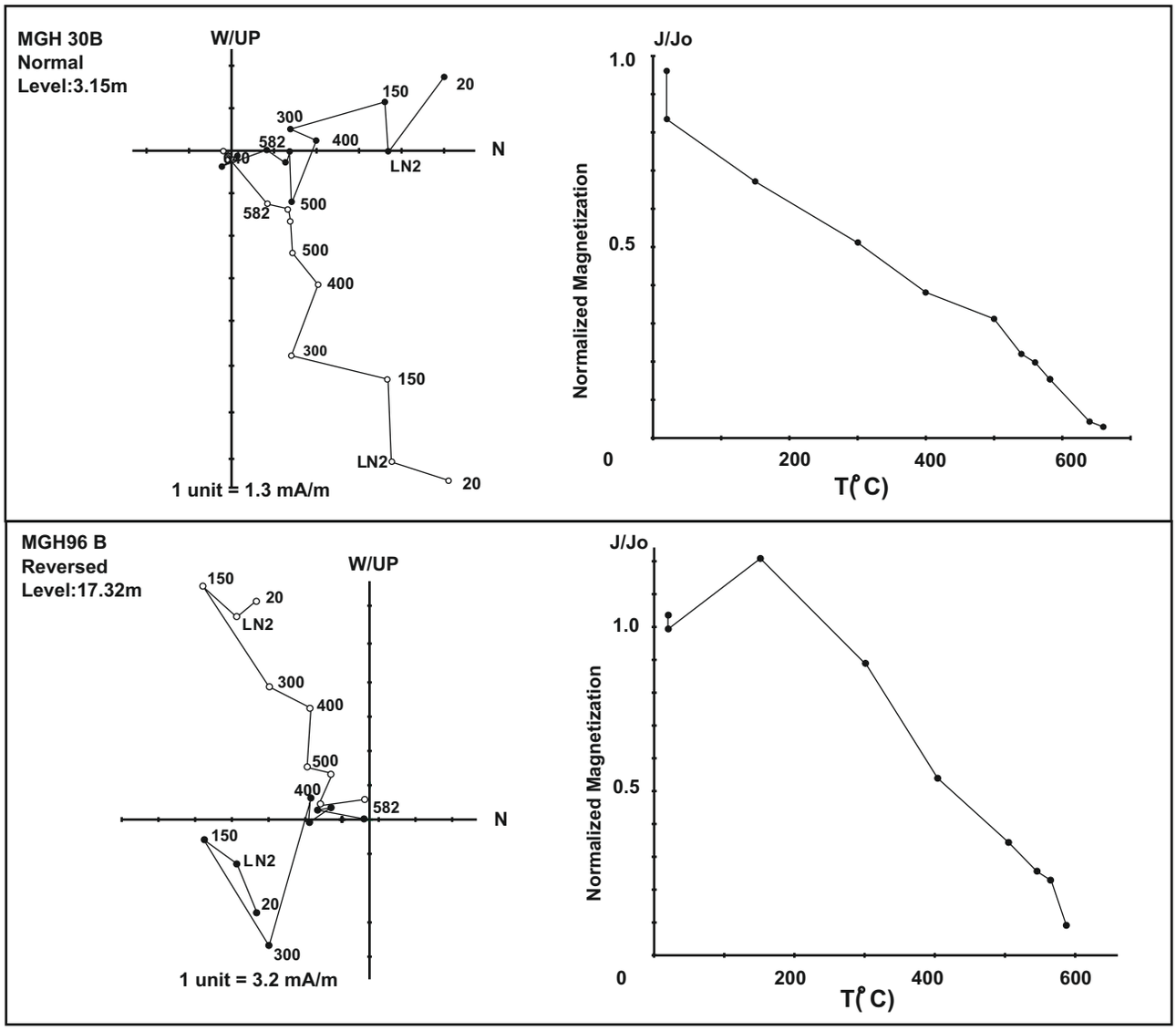
MGH 30B
Normal
Level:3.15m
W/UP
N
150
20
300
582
400
LN2
500
582
500
400
300
150
LN2
20
1 unit = 1.3 mA/m
J/Jo
1.0
0.5
0
Normalized Magnetization
200
400
600
T(°C)
MGH96 B
Reversed
Level:17.32m
W/UP
150
20
LN2
300
400
500
400
582
N
150
LN2
20
300
1 unit = 3.2 mA/m
J/Jo
1.0
0.5
0
Normalized Magnetization
200
400
600
T(°C)

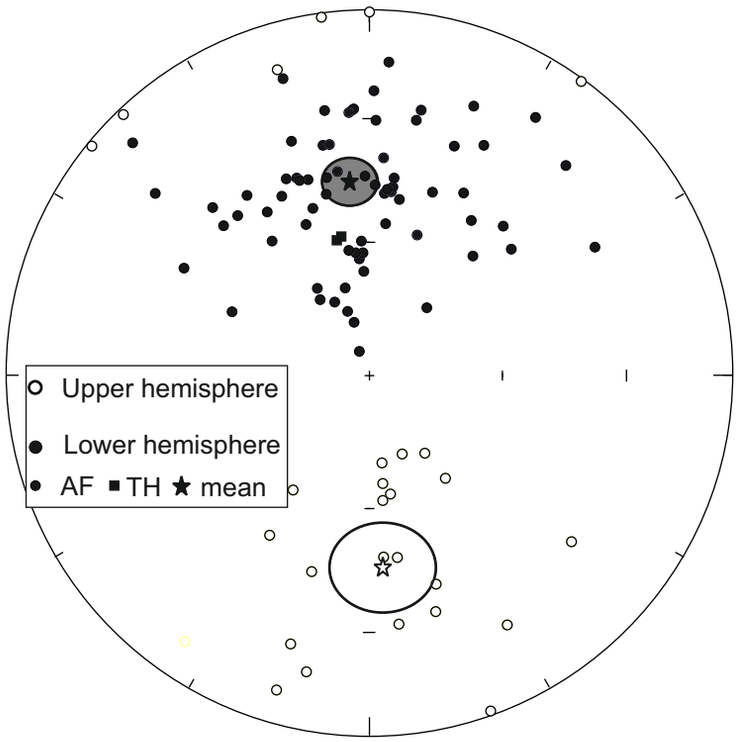
Upper hemisphere
Lower hemisphere
AF
TH
mean

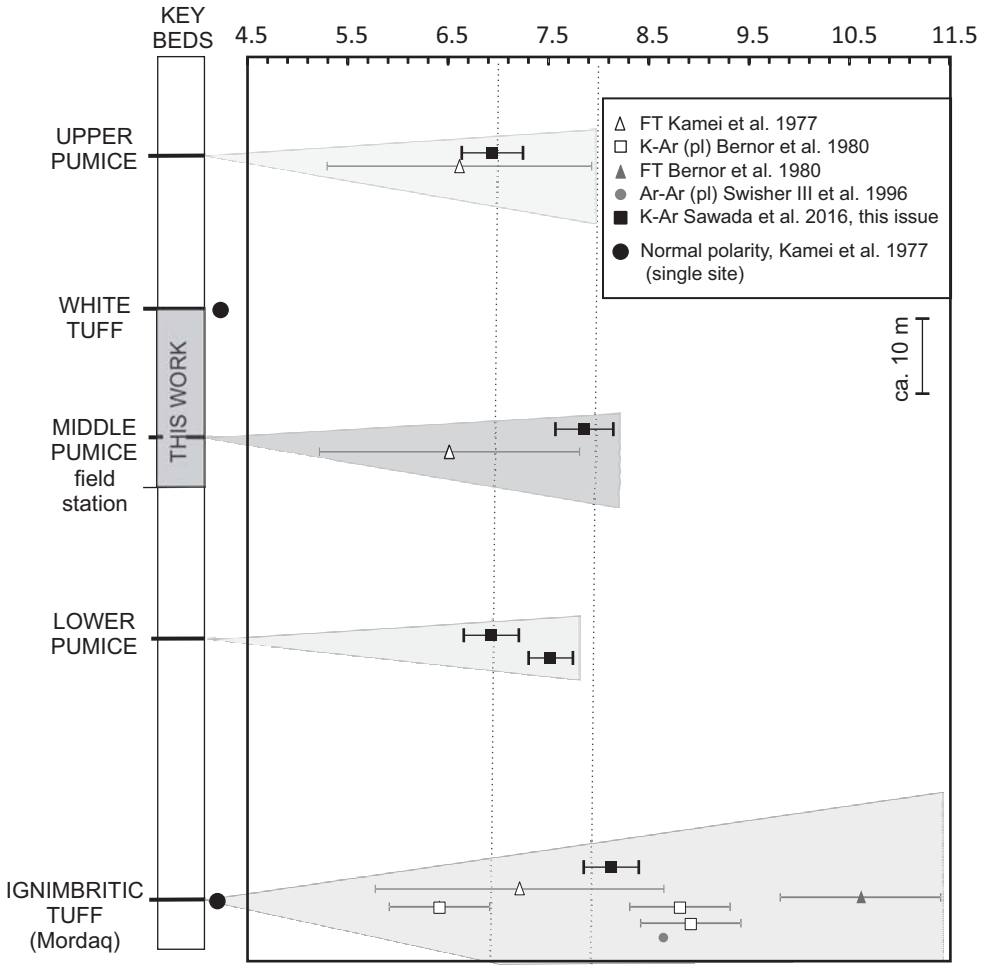
KEY BEDS
4.5
5.5
6.5
7.5
8.5
9.5
10.5
11.5
UPPER PUMICE
WHITE TUFF
MIDDLE PUMICE field station
LOWER PUMICE
IGNIMBRITIC TUFF (Mordaq)
THIS WORK
FT Kamei et al. 1977
K-Ar (pl) Bernor et al. 1980
FT Bernor et al. 1980
Ar-Ar (pl) Swisher III et al. 1996
K-Ar Sawada et al. 2016, this issue
Normal polarity, Kamei et al. 1977 (single site)
ca. 10 m